



# Effectiveness of Antiviral Therapy in Highly-Transmissible Variants of SARS-CoV-2: A Modeling and Simulation Study

Verena Schöning<sup>1†</sup>, Charlotte Kern<sup>1,2†</sup>, Carlos Chaccour<sup>3,4,5</sup> and Felix Hammann<sup>1\*</sup>

<sup>1</sup>Clinical Pharmacology and Toxicology, Department of General Internal Medicine, Inselspital, Bern University Hospital, University of Bern, Bern, Switzerland, <sup>2</sup>Graduate School for Health Sciences, University of Bern, Bern, Switzerland, <sup>3</sup>Department of Microbiology and Infectious Diseases, Clínica Universidad de Navarra, Pamplona, Spain, <sup>4</sup>Centro de Investigación Biomédica en Red de Enfermedades Infecciosas, Madrid, Spain, <sup>5</sup>ISGlobal, Hospital Clinic, University of Barcelona, Barcelona, Spain

## OPEN ACCESS

### Edited by:

Qing Xia,  
Peking University, China

### Reviewed by:

Richard K. Plemper,  
Georgia State University,  
United States  
Alejandro Hernan Gonzalez,  
Consejo Nacional de Investigaciones  
Científicas y Técnicas (CONICET),  
Argentina

### \*Correspondence:

Felix Hammann  
felix.hammann@insel.ch

<sup>†</sup>These authors have contributed  
equally to this work and share first  
authorship

### Specialty section:

This article was submitted to  
Experimental Pharmacology and Drug  
Discovery,  
a section of the journal  
Frontiers in Pharmacology

Received: 16 November 2021

Accepted: 17 January 2022

Published: 09 February 2022

### Citation:

Schöning V, Kern C, Chaccour C and  
Hammann F (2022) Effectiveness of  
Antiviral Therapy in Highly-  
Transmissible Variants of SARS-CoV-  
2: A Modeling and Simulation Study.  
Front. Pharmacol. 13:816429.  
doi: 10.3389/fphar.2022.816429

As of October 2021, neither established agents (e.g., hydroxychloroquine) nor experimental drugs have lived up to their initial promise as antiviral treatment against SARS-CoV-2 infection. While vaccines are being globally deployed, variants of concern (VOCs) are emerging with the potential for vaccine escape. VOCs are characterized by a higher within-host transmissibility, and this may alter their susceptibility to antiviral treatment. Here we describe a model to understand the effect of changes in within-host reproduction number  $R_0$ , as proxy for transmissibility, of VOCs on the effectiveness of antiviral therapy with molnupiravir through modeling and simulation. Molnupiravir (EIDD-2801 or MK 4482) is an orally bioavailable antiviral drug inhibiting viral replication through lethal mutagenesis, ultimately leading to viral extinction. We simulated 800 mg molnupiravir treatment every 12 h for 5 days, with treatment initiated at different time points before and after infection. Modeled viral mutations range from 1.25 to 2-fold greater transmissibility than wild type, but also include putative co-adapted variants with lower transmissibility (0.75-fold). Antiviral efficacy was correlated with  $R_0$ , making highly transmissible VOCs more sensitive to antiviral therapy. Total viral load was reduced by up to 70% in highly transmissible variants compared to 30% in wild type if treatment was started in the first 1–3 days post inoculation. Less transmissible variants appear less susceptible. Our findings suggest there may be a role for pre- or post-exposure prophylactic antiviral treatment in areas with presence of highly transmissible SARS-CoV-2 variants. Furthermore, clinical trials with borderline efficacious results should consider identifying VOCs and examine their impact in post-hoc analysis.

**Keywords:** COVID-19, SARS-CoV-2 variants, variants of concern (VOCs), mathematical disease modeling, molnupiravir, viral kinetic modelling, paxlovid, pharmacometrics

## INTRODUCTION

With now almost 2 years into the COVID-19 pandemic caused by SARS-CoV-2 there have been abundant drug repurposing efforts. Unfortunately, neither established agents (e.g., hydroxychloroquine) nor experimental drugs have lived up to their initial promise. In fact, only corticosteroids appear to have limited benefits, and then only on the all-cause mortality and need for

mechanical ventilation outcomes in severe cases (Siemieniuk et al., 2020). As vaccines are being rolled out worldwide, new virus variants continue to take hold, some of which harbor the potential for vaccine escape (diminished effectiveness of vaccines developed against wild type strains) (Wang et al., 2021). There are indications that immunity acquired during the natural course of a SARS-CoV-2 infection is similarly reduced (Andreano et al., 2021).

Most notorious amongst these variants of concern (VOCs) are five lineages, now termed Alpha through Delta and Omicron (lineages B.1.1.7, B.1.351, P.1, B.1.617.2, and B.1.1.529, respectively). While they were first detected in late 2020 through November 2021, they are assumed to have been circulating for much longer (Rambaut et al., 2020; Tegally et al., 2020; Faria et al., 2021). A hallmark feature of those VOCs is their high transmissibility, in part caused by mutations such as N501Y in the spike protein, resulting in greater affinity for the ACE2 receptor (Baric, 2020).

Public health measures like physical distancing, wearing of personal protective equipment, and stay-at-home orders implemented during outbreaks of wild type strains have contributed to reducing overall transmission, but failed, at least partially, to contain the spread of variants as effectively. First reports of waning vaccine immunity (Goldberg et al., 2021) and mutations compromising vaccine efficacy are appearing, causing disruption to national vaccination strategies, and treatment with convalescent plasma may even select for mutations and new variants (Cohen, 2021; Planas et al., 2021). It is apparent that other preventive measures such as drug-based primary or post-exposure prophylaxis still need to be explored, particularly if viral loads are already high in pre-symptomatic individuals, leading to greater infectiousness (Jones et al., 2021).

The treatment options for COVID-19 appear limited so far, but several antiviral drugs are under consideration. Gilead's remdesivir, an adenosine nucleotide analog acting as a RNA chain terminator, hence inhibiting viral replication, has been granted emergency use authorization by the FDA for the treatment of COVID-19 patients, with a daily intravenous administration (FDA, 2020). However, the ISARIC WHO study of United Kingdom hospitalized patients with COVID-19, where adults with severe COVID-19 were treated with remdesivir, showed that treatment was not associated with a reduction in mortality (Arch et al., 2021).

Of the many novel antivirals being proposed, two are currently receiving widespread attention. The first, Paxlovid, is a combination of the Pfizer compound PF-07321332 and ritonavir as a pharmacokinetic booster, and acts as an inhibitor of SARS-CoV-2-3-CL protease, thereby reducing viral replication. It has no marketing authorization yet, but preliminary results are promising and show reduction of risk for COVID-19 related hospital admission or death in phase II-III EPIC-HR clinical trials (Mahase, 2021b).

The second, molnupiravir (EIDD-2801 or MK-4482), developed by Merck and Ridgeback, is a nucleoside analog much like remdesivir, but brings with it the advantage of being available as an oral formulation. Molnupiravir is the prodrug (5'-isobutyric ester form) of the nucleoside analog  $\beta$ -D-N<sup>4</sup>-

hydroxycytidine (NHC or EIDD-1931) (Painter et al., 2019). Molnupiravir is cleaved in the plasma to liberate NHC. NHC is then phosphorylated in the cell by host kinases to its active form NHC triphosphate (EIDD-2061). The viral RNA-dependent RNA polymerase (RdRp) then inserts the non-functional NHC triphosphate instead of uridine triphosphate. When the resulting RNA is used as template, NHC can form stable base pairs with either guanidine or adenine, leading to what has been termed 'lethal mutagenesis' (Kabinger et al., 2021; Malone and Campbell, 2021). *In vitro*, NHC showed an inhibitory effect on SARS-CoV-2 replication in Calu-3 cells, a disease-relevant human lung epithelial cell line, and *in vivo* in a Syrian hamster model (Rosenke et al., 2021). An *in vivo* study in a ferret model showed that, depending on timing of treatment initiation of molnupiravir, the viral replication of SARS-CoV-2 could be completely silenced within hours to days. Furthermore, the transmission to uninfected contact animals could be prevented (Cox et al., 2021). These results were corroborated by a study in human lung-only mice, where molnupiravir also markedly inhibited SARS-CoV-2 replication (Wahl et al., 2021). News releases from Merck suggest that molnupiravir is safe in human subjects and that as per interim analysis reduced the risk of hospitalization or death by approximately 50% in patients at risk (Mahase, 2021a).

With this study, we aim to better understand the influence of adaptations in SARS-CoV-2 pathobiology on drug development and treatment. For this, we simulated the impact of changes of within-host reproduction number  $R_0$ , as proxy for within-host transmissibility, on antiviral treatment efficacy. For this purpose, we used a recent model of within-host viral kinetics trained on load profiles from Singapore obtained in early 2020 (Kern et al., 2021), and combined it with a pharmacometric model to simulate treatment with molnupiravir as a representative of novel experimental antivirals currently under investigation for the treatment of COVID-19. We then modified  $R_0$  in the viral kinetics model and assessed the effects on within-host viral dynamics. The assessed antiviral effect metrics are total viral load (the total amount of virions produced calculated as area under the viral load curve (AUC)), peak viral load (the highest amount of virions as maximum  $C_{t_{min}}$ ), and disease duration (time above the detection threshold, virus permanence time).

## METHODS

### Data Sources

Young et al. (2020), a study that followed 18 COVID-19 patients in four Singapore hospitals, provided the viral kinetic patient profiles. Authors used RT-PCR to determine the viral load from nasopharyngeal swabs and results were provided as cycle threshold (Ct) values. Because the correlation between Ct values and viral load changes depending on the laboratory and analytics, model output was related with observed Ct values with a published regression fit (Chu et al., 2020). An average incubation period of 5 days was chosen for all patients, because the time of infection was not recorded (Lauer et al., 2020). Positivity threshold was set at 35, corresponding to 101.58 copies/mL (Wang et al., 2020).

## Viral Kinetics Models

Viral loads were simulated from a target-cell limited model, a dynamic in-host infection model considering target cells, infected cells and virus particles (Ciupe and Heffernan, 2017). The equilibrium states, stability and characterization of different initial conditions are demonstrated in other studies (Abuin et al., 2020; 2021). We added the dynamics of an acquired immune response around 10 days post inoculation (dpi). In brief, a small amount of virus particles  $V$  are considered to infect a pool of target cells  $T$  with cellular infection rate  $\beta$ . Infected cells  $I$  produce and shed virions at a production rate  $p$  (Canini and Perelson, 2014). The rate parameters  $c$  and  $\delta$  represent viral clearance, and cell death of infected cells, respectively. The time-dependent number of target cells (Eq. 1), infected cells (Eq. 2) and circulating virions (Eq. 3) are described by the following system of ordinary differential equations:

$$\frac{dT}{dt} = -\beta TV \quad (1)$$

$$\frac{dI}{dt} = \beta TV - \delta I \quad (2)$$

$$\frac{dV}{dt} = (1 - \eta)pI - c(1 + \epsilon_{\text{immunity}})V \quad (3)$$

Acquired immunity  $\epsilon_{\text{immunity}}$  develops according to a sigmoidal  $E_{\text{max}}$  model (Eq. 4), and effects of drug treatment  $\eta$  enter dependent on their concentrations and  $IC_{50}$  or  $EC_{50}$  values for their respective targets (Eq. 5). We modeled drug treatment within an impulsive antiviral framework where  $C(t)$ , the concentration of the drug and its effects at a given time dynamically changes in accordance with the pharmacokinetics of molnupiravir (Hernandez-Mejia et al., 2020; Perez et al., 2021):

$$\epsilon_{\text{immunity}} = \frac{E_{\text{max immunity}} \times t^{\text{Hill immunity}}}{EC_{50 \text{ immunity}}^{\text{Hill immunity}} + t^{\text{Hill immunity}}} \quad (4)$$

$$\eta = \frac{E_{\text{max}} \times C(t)}{IC_{50} + C(t)} \quad (5)$$

The within-host reproduction number  $R_0$  is the amount of cells infected per infected cell. It is not a single variable in the system of ordinary differential equations used to describe the viral kinetic, but depends on the other variables. We used a modern approach for invasion analysis (Hurford et al., 2010) for calculating  $R_0$  (Eq. 6), which was already applied by another study to model Sars-CoV-2 viral kinetics (Czuppon et al., 2020):

$$R_0 = \frac{p\beta T_0}{\delta(c + \beta T_0)} \quad (6)$$

**Table 1** shows viral kinetics model parameters used. A detailed description of the model and its implementation is given in Kern et al. (2021).

## Highly Transmissible SARS-CoV-2 Variants

Highly transmissible variants were considered to have 1.25-, 1.5-, and 2-fold increases in the within-host reproductive number  $R_0$

compared to the wild type ( $R_0 = 3.79$ ). Co-adaptation (i.e., a less transmissible mutation) was accounted for by simulating a 0.75-fold decrease in  $R_0$ .

## Pharmacokinetic Models

No published population pharmacokinetics model was available for molnupiravir (EIDD-2801/MK-4482), the prodrug of NHC (EIDD-1931). The pharmacokinetic profile of NHC was extracted from a safety study in fasted healthy volunteers given single doses of 200–800 mg molnupiravir (Painter et al., 2021) with a digitizing software. We used Monolix (version 2020R1), to fit the following model to the pharmacokinetic profile: a one compartment model with linear elimination, an extravascular administration with transit compartments and first order absorption. **Table 1** shows the pharmacokinetic model parameters. We performed a non-compartmental analysis (NCA) with the resulting curve to estimate common pharmacokinetic metrics (see **Supplementary Table S2**).

Only the unbound fraction of the drug should be considered available for target engagement. To date, no plasma protein binding values are available for molnupiravir or NHC. Since NHC has a structure close to cytidine and cytidine in turn has a similar structure to cytosine arabinoside (Ara-C), we used findings from a study on the interaction of Ara-C with human plasma proteins, where 13.3% of Ara-C in the plasma was bound to proteins (van Prroijen et al., 1977). The effective drug concentrations were reduced accordingly for simulations of drug effects.

In addition to protein binding, organ distribution also needs to be considered. We used literature-based approximations to adjust for differences between plasma and lung concentration profiles. Murine pharmacokinetics of NHC and the active form NHC triphosphate (EIDD-2061) after an oral dose of 500 mg/kg NHC has been described by Painter et al. (2019). Concentration curves were available in mice spleen, brain, heart, kidney, liver and lung for NHC and the activated metabolite. After extracting the curves for each organ, PK parameters (AUC,  $C_{\text{max}}$ ,  $T_{\text{max}}$ ) were computed. For the lung,  $C_{\text{max}}$  for NHC (EIDD-1931) was 47.99 nmol/g and for NHC triphosphate (EIDD-2061) was 7.87 nmol/g. The metabolite/parent drug ratio (NHC triphosphate/NHC) was 0.164, and was used to estimate the available concentrations of active metabolite over time.

## Pharmacodynamic Effects

The effectiveness of NHC was shown *in vitro* in Calu-3 cells (human lung epithelial cell line) by Rosenke et al. (2021), after 24 h of treatment with NHC. An  $IC_{50}$  of 0.4146  $\mu\text{M}$  was used in the simulations as an inhibitory influence on viral production  $p$ , as molnupiravir inhibits viral replication. The proposed dosing regimen was molnupiravir 800 mg every 12 h for 5 days (Merck Sharp & Dohme Corp, 2020).

## Software

Pharmacokinetics data for NHC and NHC triphosphate was read out with WebPlotDigitizer (version 4.2, <https://automeris.io/WebPlotDigitizer>). Corresponding pharmacokinetic profiles were modelled in Monolix (version 2020R1, <http://www.lixoft>).

**TABLE 1 |** Viral kinetics and molnupiravir pharmacokinetic model parameters. The pharmacokinetic profile of NHC was extracted from a safety study in fasted healthy volunteers given a single dose of 800 mg molnupiravir (Painter et al., 2021) with a digitizing software. A one compartment model with transit absorption and linear elimination was fitted to the pharmacokinetic profile. \*IC<sub>50</sub> value for NHC (EIDD-1931) inhibition of SARS-CoV-2 replication in human lung epithelial Calu-3 cells after 24 h treatment.

Parameter	Definition	Value	Reference
Within-host viral kinetics			
$\beta$	Cellular infection rate	$\beta = \frac{R_0 c \delta}{T_0 (\rho - R_0 \delta)}$	Calculated
$\delta$	Infected cell death rate	0.54 day <sup>-1</sup>	Estimated
$\rho$	Viral production rate	10.2 (copies/mL) day <sup>-1</sup> cell <sup>-1</sup>	Estimated
$c$	Viral clearance	5.07 day <sup>-1</sup>	Estimated
$R_0$	Within-host reproduction number	3.79	Li et al. (2020)
$T_0$	Initial target cells	10 <sup>6</sup> cells	Fixed by authors
$V_0$	Initial virus load (inoculum)	10 <sup>0</sup> virions	Fixed by authors
$EC_{50, \text{immunity}}$	Half maximal effective concentration for immune response	10.2	Estimated Long et al. (2020)
$Hill_{\text{immunity}}$	Slope of dose-response curve	3.4	Estimated Long et al. (2020)
$E_{\text{max, immunity}}$	Maximum effect on viral clearance	57.0	Estimated
Pharmacokinetics of molnupiravir			
Ktr	Transit absorption rate	2.01 h <sup>-1</sup>	Estimated
Mtt	Mean transit time	0.64 h	Estimated
ka	Absorption rate constant	2.01 h <sup>-1</sup>	Estimated
V	Central compartment volume	0.052 L	Estimated
Cl	Clearance	0.11 L/h	Estimated
*IC <sub>50</sub>	Half maximal inhibitory concentration	0.4146 $\mu$ M	Rosenke et al. (2021)
PPB	Plasma protein binding	13.3%	Estimated van Prooijen et al. (1977)

com, Antony, France) and simulated in GNU R (version 3.6.3, R Foundation for Statistical Computing, <http://www.R-project.org>, Vienna, Austria), with the corresponding R package mlxR (version 4.1.3). PK parameters for the mice organs were calculated in the Non Compartmental Analysis framework of PKanalix (version 2020R1, <http://www.lixoft.com>, Antony, France). Data analysis and visualization were performed with GNU R. Ordinary differential equation (ODE) systems were implemented with the R package deSolve (version 1.28).

## RESULTS

The viral load profiles of 13 untreated patients [from (Young et al., 2020)] were best described by a standard target cell limited model. Death rate of infected cells  $\delta$ , viral production rate  $\rho$ , viral clearance  $c$ , and maximum immune effect on clearance  $E_{\text{max, immunity}}$  were estimated from the individual profiles with the Nelder-Mead method and then averaged (Kern et al., 2021). The pharmacokinetics of molnupiravir based on digitalized plasma concentration curves, estimated from clinical trial data analysis, have a satisfactory fit with the information provided in Painter et al. (2021) (see **Supplementary Figure S1**). **Table 1** contains the final viral kinetics and molnupiravir pharmacokinetics model parameter estimates.

Viral load dynamics using wild type ( $R_0^*1$ ) parameterizations served as the baseline for comparison. Viral loads reach positivity ( $C_t < 35$ ) after 5.4 days. Positivity is maintained for a total duration of 13.5 days, and the viral load peak of 28.4  $C_{t_{\text{min}}}$  appears after 8.1 days (Kern et al., 2021). Compared to wild type strains, increases in within-host  $R_0$  up to two-fold

transmissibility resulted in earlier positivity (2.1–3.7 dpi vs. 5.4 dpi in wild type). Higher viral load peaks ( $C_{t_{\text{min}}}$  25.2–27.4 vs. 28.4 in wild type) are achieved earlier after inoculation (4.5–6.3 vs. 8.1 days in wild type) and, while reduced, durations below the  $C_t$  threshold of 35 are comparable (11.4–12.7 vs. 13.5 days in wild type). Total viral load [area under the viral load curve (AUC)] increased 152–402% in comparison to wild type. Co-adaptation to 75% the original  $R_0$  was predicted to result in a later positivity at 9.1 dpi with a prolonged duration of 15.1 days, a lower viral load peak of  $C_{t_{\text{min}}}$  29.6 at 11.9 days, and a reduced viral load AUC (66%). Simulated profiles are shown in **Figure 1**; **Table 2**.

The treatment effects of molnupiravir are modeled within an impulsive antiviral framework. Molnupiravir 800 mg is administered every 12 h for 5 days, however, the concentration needed for antiviral activity within in the model cannot be sustained over the time between administrations based on the  $EC_{50}$  applied and the pharmacokinetic parameters. Therefore, effects of drug treatments are visible in the viral load curve by repeated sharp decreases and increases of viral load (see **Supplementary Figure S2**).

Treatment with molnupiravir 800 mg every 12 h for 5 days in wild type ( $R_0^*1$ ) leads to a reduced total viral load and peak viral load down to 68% and 0.8 log units, respectively. Treatment initiation before five dpi resulted in a delayed positivity (i.e., meeting the detectability criterion of  $C_t < 35$ ). In addition, the total duration was shorter if treatment was initiated before five dpi, and longer if initiated later. These treatment effects were sensitive to changes in  $R_0$  (**Figure 2**). Higher transmissibility was positively correlated with a greater reduction in total viral load, peak viral load and

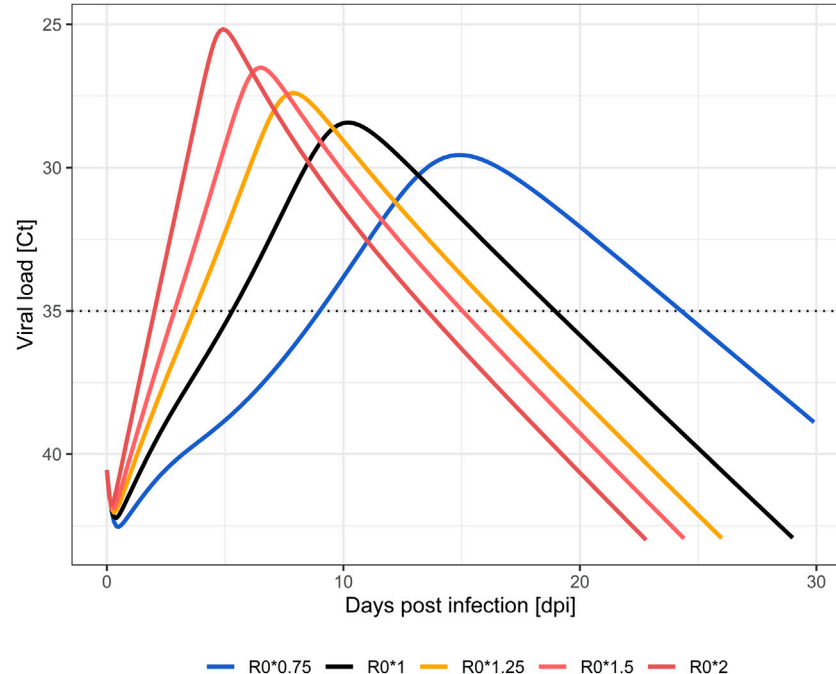


**FIGURE 1** | Simulated viral load profiles by change in within-host infectivity ( $R_0$ ). Wild type SARS-CoV-2 strain (black), less transmissible (blue), highly transmissible (orange to red) variants. Limit of quantification ( $C_t = 35$ ) is displayed as a dotted line.

**TABLE 2** | Simulated within-host viral kinetics at different levels of cellular infectivity (given as multiples of  $R_0 = 3.79$ ). Abbreviations: days post infection (dpi); day (d); minimum serial cycle threshold values ( $C_{t_{min}}$ ); time of  $C_{t_{min}}$  ( $T_{max}$ ); area under the curve (AUC); percentage difference in AUC compared to wild-type ( $\Delta AUC\%$ ).

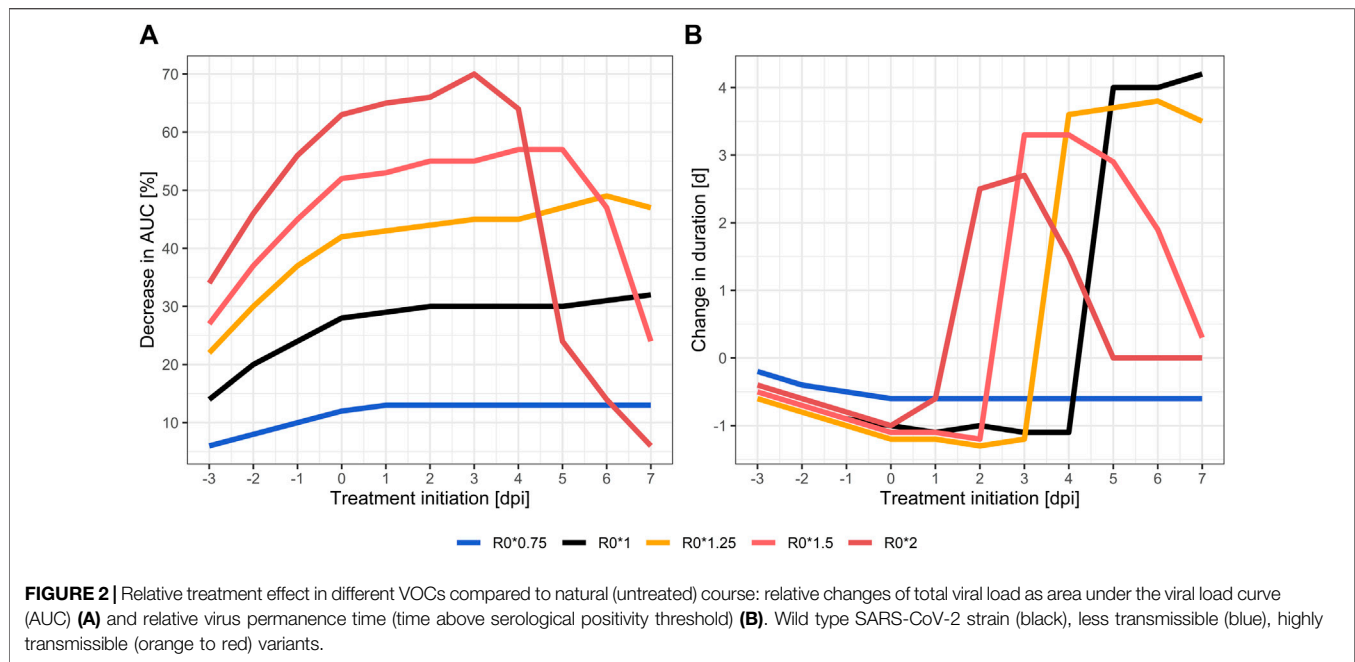
Infectivity	Start positivity [dpi]	Duration [d]	$C_{t_{min}}$	$T_{max}$	AUC [d*log (copies/mL)]	$\Delta AUC\%$
Wild type						
$R_0$	5.4	13.5	28.4	8.1	12003	100
Highly transmissible mutation						
$R_0*1.25$	3.7	12.7	27.4	6.3	18278	152
$R_0*1.5$	2.9	12.1	26.5	5.4	26648	222
$R_0*2$	2.1	11.4	25.2	4.5	48197	402
Less transmissible mutation						
$R_0*0.75$	9.1	15.1	29.6	11.9	7975	66

delayed time to positivity when treated early. Compared to untreated courses, the total viral load is reduced to 51% ( $R_0*1.25$ ) or 30% ( $R_0*2$ ) in the highly-transmissible variants.  $C_{t_{min}}$  levels were reduced by more than two log units in  $R_0*2$  (27.7 vs. 25.2 untreated) and viral peak loads were reached at a later time point. Duration was less sensitive to changes in  $R_0$ , with a tendency towards prolonged positivity with increasing  $R_0$  ( $R_0*1.25$ : 16.5 vs. 12.7 days untreated,  $R_0*2$ : 14.1 vs. 11.4 days untreated). Furthermore, the treatment effects were not only influenced by transmissibility, but also by timing of treatment initiation, i.e. a higher the transmissibility requires an earlier treatment initiation. Later treatment initiation diminishes the antiviral effect of the treatment quickly. In less transmissible variants, the

positive treatment effects were less pronounced. The total viral load and peak viral load were only reduced by up to 13% and 0.1 log units, respectively. On the other hand, the time windows for maximal treatment effect were wider, and later treatment initiation therefore did not sacrifice much efficacy (**Supplementary Table S1**).

## DISCUSSION

With this modeling and simulation analysis of SARS-CoV-2 variants, we show the potential influence of altered within-host transmissibility on patient viral load dynamics. While the study is *in silico* and not based on *in vivo* data, the results suggest



that patients infected with a VOC are likely to experience shorter, but stronger exposures to virions with higher peak loads. This is confirmed by a recent publication, which showed that patients infected with the Delta variant had approximately 1'000-fold higher viral loads than what was seen in earlier 19A/19B strains (Li et al., 2021). Similar evidence exists also for other VOCs (Frampton et al., 2021).

Early treatment of SARS-CoV-2 infections achieved the greatest effect on total viral load and peak load, independently from the antiviral treatment studied, as previously noted (Goncalves et al., 2020; Kim et al., 2020; Kern et al., 2021). As time of treatment initiation nears the peak of viral loads when untreated, when most of the susceptible target cells are already infected, antiviral effect is increasingly attenuated. This can be seen in the steep decline of impact on total viral load in **Figure 2**. The more target cells are already infected due to a delayed treatment initiation, the less intracellular viral replications can be prevented by the antiviral treatment. This effect is accentuated in highly transmissible VOCs, which appear to be even more susceptible to an early initiation of antiviral treatment. The higher transmissibility of VOC leads to a quicker infection of all target cells, which can be seen as steep ascent in **Figure 1**. Consequentially, positivity in RT-PCR testing in highly transmissible VOC is expected to be achieved about 3 days sooner than in wild type, also the peak viral concentrations is reached earlier (see **Supplementary Table S1**). Due to the high viral replication dynamic, especially in the early days of infection, the simulation predicts that a timely initiated antiviral treatment is more effective than in variants with low transmissibility, i.e., a lower viral replication dynamic. Support for this is seen in the manufacturer's early termination of the inpatient part of placebo-controlled phase II/III dose-finding trials (MOVE-IN in inpatients, and MOVE-OUT in outpatients) out of lack of

efficacy (Merck, 2021a). MOVE-out, on the other hand, which was halted after an interim analysis of 775 patients, found a reduction of risk for hospitalization or death from 14.1 to 7.3% in at-risk, non-hospitalized adult patients with mild-to-moderate COVID-19 (number needed to treat = 15) (Merck, 2021b).

Containing the COVID-19 pandemic requires multiple strategies, including vaccination, prophylaxis and treatment, combined with diagnostic, quarantine and contact tracing, in addition to protective measures like social distancing, mask wearing and hand hygiene. Any delay in making a decision-to-treat because of lack of symptoms or availability of diagnostic reports may result in worse outcomes. Possible scenarios include pre-exposure prophylaxis in isolated outbreaks or post-exposure prophylaxis for at-risk contacts of SARS-CoV-2 positive patients, e.g., specific settings such as residential homes, in immunosuppressed people, or localized outbreaks. However, rapid diagnostics combined with contact-tracing strategies may provide a more realistic alternative to treatment of outpatients before the onset of clinical symptoms.

Furthermore, the impulsive effects of the antiviral treatment in our model oscillates between complete suppression of viral replication to no antiviral effect. Provided that an actual population pharmacokinetics had been available, it be possible to optimize the treatment schedule, as shown for the treatment of influenza A with zanamivir (Hernandez-Mejia et al., 2020).

Several limitations need to be considered. Measurements of viral dynamics neither directly translate to clinical courses nor to individual infectiousness, though such correlations have been described (Fajnzyblber et al., 2020; He et al., 2020). We simulated from a model that accounts for acquired immune response as described in mid 2020 in patients from hospitals in Chongqing (near Hubei Province). Immunogenicity of VOCs may differ, as may the response of other populations. Additionally, predicting

the effects of prophylaxis is difficult with the type of model employed here as extinction (complete disappearance of virions from the system) is a fringe case. We modelled the population pharmacokinetics of molnupiravir based on digitalized plasma concentration curves, as no other information was publicly available. Even though pharmacokinetic parameters estimated from actual trial data analysis are bound to be more precise, the resulting curves fit well with the information provided in (Painter et al., 2021). As we used molnupiravir as exemplary drug to analyse the interaction of VOCs and antiviral treatment, slight changes in the pharmacokinetic parameters might result in different AUC, peak load and duration values, but do not change the overall conclusion of the study.

Published versions of molnupiravir clinical trial protocols do not provide information on pharmacokinetic distribution parameters such as protein binding or transporter interactions. We assumed protein binding to only marginally limit the availability of free drug (similar to structure analogues or nucleoside reverse transcriptase inhibitors used for other indications such as HIV/AIDS) (Ridgeback Biotherapeutics, 2020). Cellular uptake of nucleosides is transporter-dependent (Pastor-Anglada and Pérez-Torras, 2018), and this might also limit the concentration of the active substance of molnupiravir within the respiratory tissue: in a mouse model, the concentration of NHC-triphosphate plateaued at 10 nmol/g lung tissue, even at higher plasma concentrations (Yoon et al., 2018). No comparable data are available in humans, so it remains unclear whether a saturation effect is observable in human lung tissue at the recommended clinical doses. As a consequence, should a relevant plateau effect exist, the model may overestimate molnupiravir efficacy. However, this limitation only applies to our model, as clinical data have shown the efficacy of molnupiravir (Mahase, 2021a), suggesting sufficient tissue concentrations.

The authors would like to stress that molnupiravir was used as a model drug to study the effects on altered within-host infectivity in SARS-CoV-2, not as an endorsement for its use or proof of its clinical efficacy as a prophylactic drug or treatment in manifest cases. We ran comparable simulations with Paxlovid, which also inhibits viral replication, and obtained comparable results (data not shown) with regards to within-host viral dynamics and antiviral drug efficacy. Even though we were not able to model remdesivir, another inhibitor of viral replication, we assume that changes in transmissibility may lead to similar changes in within-host viral dynamics and antiviral drug efficacy.

Apart from focusing efforts on early treatment, running clinical trials should account for variants in trial design and analysis. Given that many trials have included subjects during a time when the now discovered VOCs had already been circulating, it could be worthwhile to revisit borderline efficacious drugs and screen patient samples for these mutant strains in order to perform subgroup analyses, focusing on responders vs. non-responders. This may uncover significant effects against certain variants even when no effect was

seen on trial level. Additionally, clinical trials should consider a subgroup analysis based on days after symptom onset before treatment initiation, as this influences the efficacy of the treatment. This would also improve the comparability of different antiviral clinical trials, if the inclusion criteria vary in this point. If successful, this would open up additional avenues for early treatment or prophylaxis that could complement vaccine campaigns in areas of high VOC prevalence, especially as long as these are still suffering from production shortages and supply chain problems. Furthermore, the problem of vaccine resistance and escape should be considered because it can negatively affect public health, as vaccination campaigns could retroactively be rendered ineffective. With case incidences on the rise again even in populations with high vaccine coverage, prophylactic treatment could help prevent hospital overcrowding.

## DATA AVAILABILITY STATEMENT

The original contributions presented in the study are included in the article/**Supplementary Material**, further inquiries can be directed to the corresponding author. The source code is available on GitHub: <https://github.com/cptbern/sars2-variants>.

## AUTHOR CONTRIBUTIONS

VS: formal analysis, investigation, methodology, software, visualisation, writing; CK: formal analysis, investigation, methodology, software, visualisation, writing; CC: validation, funding acquisition, writing; FH: conceptualisation, formal analysis, funding acquisition, methodology, software, supervision, validation, visualisation, writing—original draft. All authors contributed to the final version.

## FUNDING

VS, CK, CC, and FH received salary support from Unitaid through the BOHEMIA grant to ISGlobal. ISGlobal acknowledges support from the Spanish Ministry of Science and Innovation through the “Centro de Excelencia Severo Ochoa 2019-2023” Program (CEX 2018-000806-S), and support from the Generalitat de Catalunya through the CERCA Program.

## SUPPLEMENTARY MATERIAL

The Supplementary Material for this article can be found online at: <https://www.frontiersin.org/articles/10.3389/fphar.2022.816429/full#supplementary-material>

## REFERENCES

- Abuin, P., Anderson, A., Ferramosca, A., Hernandez-Vargas, E. A., and Gonzalez, A. H. (2020). Characterization of SARS-CoV-2 Dynamics in the Host. *Annu. Rev. Control.* 50, 457–468. doi:10.1016/j.arcontrol.2020.09.008
- Abuin, P., Anderson, A., Ferramosca, A., Hernandez-Vargas, E. A., and Gonzalez, A. H. (2021). Dynamical Characterization of Antiviral Effects in COVID-19. *Annu. Rev. Control.* 52, 587–601. doi:10.1016/j.arcontrol.2021.05.001
- Andreano, E., Piccini, G., Licastro, D., Casalino, L., Johnson, N. V., Paciello, I., et al. (2021). SARS-CoV-2 Escape from a Highly Neutralizing COVID-19 Convalescent Plasma. *Proc. Natl. Acad. Sci. USA* 118, e2103154118. doi:10.1073/pnas.2103154118
- Arch, B., Kovacs, D., Scott, J., Jones, A., Harrison, E., Rosala-Hallas, A., et al. (2021). Evaluation of the Effectiveness of Remdesivir in Treating Severe COVID-19 Using Data from the ISARIC WHO Clinical Characterisation Protocol UK: A Prospective, National Cohort Study. *medRxiv* [Preprint]. doi:10.1101/2021.06.18.21259072
- Baric, R. S. (2020). Emergence of a Highly Fit SARS-CoV-2 Variant. *N. Engl. J. Med.* 383, 2684–2686. doi:10.1056/NEJMcibr2032888
- Canini, L., and Perelson, A. S. (2014). Viral Kinetic Modeling: State of the Art. *J. Pharmacokinet. Pharmacodyn.* 41, 431–443. doi:10.1007/s10928-014-9363-3
- Chu, D. K. W., Pan, Y., Cheng, S. M. S., Hui, K. P. Y., Krishnan, P., Liu, Y., et al. (2020). Molecular Diagnosis of a Novel Coronavirus (2019-nCoV) Causing an Outbreak of Pneumonia. *Clin. Chem.* 66, 549–555. doi:10.1093/clinchem/hvaa029
- Ciupre, S. M., and Heffernan, J. M. (2017). In-Host Modeling. *Infect. Dis. Model.* 2, 188–202. doi:10.1016/j.idm.2017.04.002
- Cohen, J. (2021). South Africa Suspends Use of AstraZeneca's COVID-19 Vaccine after it Fails to Clearly Stop Virus Variant. *Science* [Online]. Available: <https://www.sciencemag.org/news/2021/02/south-africa-suspends-use-astrazenecas-covid-19-vaccine-after-it-fails-clearly-stop> (Accessed FEB 09, 2021). doi:10.1126/science.abg9559
- Cox, R. M., Wolf, J. D., and Plemper, R. K. (2021). Therapeutically Administered Ribonucleoside Analogue MK-4482/EIDD-2801 Blocks SARS-CoV-2 Transmission in Ferrets. *Nat. Microbiol.* 6, 11–18. doi:10.1038/s41564-020-00835-2
- Czuppon, P., Débarre, F., Gonçalves, A., Tenaillon, O., Perelson, A. S., Guedj, J., et al. (2020). Predicted success of Prophylactic Antiviral Therapy to Block or Delay SARS-CoV-2 Infection Depends on the Targeted Mechanism. *medRxiv* [Preprint]. doi:10.1101/2020.05.07.20092965
- Fajnzylber, J., Regan, J., Coxen, K., Corry, H., Wong, C., Rosenthal, A., et al. (2020). SARS-CoV-2 Viral Load Is Associated with Increased Disease Severity and Mortality. *Nat. Commun.* 11, 5493. doi:10.1038/s41467-020-19057-5
- Faria, N. R., Morales Claro, I., Candido, D., Franco, L. a. M., Andrade, P. S., Coletti, T. M., et al. (2021). Genomic Characterisation of an Emergent SARS-CoV-2 Lineage in Manaus: Preliminary Findings. [Online]. Available at: <https://virological.org/t/genomic-characterisation-of-an-emergent-sars-cov-2-lineage-in-manauas-preliminary-findings/586> (Accessed FEB 09, 2021).
- FDA (2020). FDA Approves First Treatment for COVID-19. [Online]. Available: <https://www.fda.gov/news-events/press-announcements/fda-approves-first-treatment-covid-19> (Accessed November 15, 2021).
- Frampton, D., Rampling, T., Cross, A., Bailey, H., Heaney, J., Byott, M., et al. (2021). Genomic Characteristics and Clinical Effect of the Emergent SARS-CoV-2 B.1.1.7 Lineage in London, UK: a Whole-Genome Sequencing and Hospital-Based Cohort Study. *Lancet Infect. Dis.* 21, 1246–1256. doi:10.1016/S1473-3099(21)00170-5
- Goldberg, Y., Mandel, M., Bar-On, Y. M., Bodenheimer, O., Freedman, L., Haas, E. J., et al. (2021). Waning Immunity after the BNT162b2 Vaccine in Israel. *New Engl. J. Med.* 385, e85. doi:10.1056/nejmoa2114228
- Gonçalves, A., Bertrand, J., Ke, R., Comets, E., De Lamballerie, X., Malvy, D., et al. (2020). Timing of Antiviral Treatment Initiation Is Critical to Reduce SARS-CoV-2 Viral Load. *CPT Pharmacometrics Syst. Pharmacol.* 9, 509–514. doi:10.1002/psp4.12543
- He, X., Lau, E. H. Y., Wu, P., Deng, X., Wang, J., Hao, X., et al. (2020). Temporal Dynamics in Viral Shedding and Transmissibility of COVID-19. *Nat. Med.* 26, 672–675. doi:10.1038/s41591-020-0869-5
- Hernandez-Mejia, G., Alanis, A. Y., Hernandez-Gonzalez, M., Findeisen, R., and Hernandez-Vargas, E. A. (2020). Passivity-Based Inverse Optimal Impulsive Control for Influenza Treatment in the Host. *IEEE Trans. Contr. Syst. Technol.* 28, 94–105. doi:10.1109/tcst.2019.2892351
- Hurford, A., Cownden, D., and Day, T. (2010). Next-generation Tools for Evolutionary Invasion Analyses. *J. R. Soc. Interf.* 7, 561–571. doi:10.1098/rsif.2009.0448
- Jones, T. C., Biele, G., Mühlemann, B., Veith, T., Schneider, J., Beheim-Schwarzbach, J., et al. (2021). Estimating Infectiousness throughout SARS-CoV-2 Infection Course. *Science* 373, eabi5273. doi:10.1126/science.abi5273
- Kabinger, F., Stiller, C., Schmitzová, J., Dienemann, C., Kokic, G., Hillen, H. S., et al. (2021). Mechanism of Molnupiravir-Induced SARS-CoV-2 Mutagenesis. *Nat. Struct. Mol. Biol.* 28, 740–746. doi:10.1038/s41594-021-00651-0
- Kern, C., Schöning, V., Chaccour, C., and Hammann, F. (2021). Modeling of SARS-CoV-2 Treatment Effects for Informed Drug Repurposing. *Front. Pharmacol.* 12, 625678. doi:10.3389/fphar.2021.625678
- Kim, K. S., Ejima, K., Ito, Y., Iwanami, S., Ohashi, H., Koizumi, Y., et al. (2020). Modelling SARS-CoV-2 Dynamics: Implications for Therapy. *medRxiv*. doi:10.1101/2020.03.23.20040493
- Lauer, S. A., Grantz, K. H., Bi, Q., Jones, F. K., Zheng, Q., Meredith, H. R., et al. (2020). The Incubation Period of Coronavirus Disease 2019 (COVID-19) from Publicly Reported Confirmed Cases: Estimation and Application. *Ann. Intern. Med.* 172, 577–582. doi:10.7326/M20-0504
- Li, C. T., Xu, J. H., Liu, J. W., and Zhou, Y. C. (2020). The Within-Host Viral Kinetics of SARS-CoV-2. *Math. Biosci. Eng.* 17, 2853–2861. doi:10.3934/mbe.2020159
- Li, B., Deng, A., Li, K., Hu, Y., Li, Z., Xiong, Q., et al. (2021). Viral Infection and Transmission in a Large Well-Traced Outbreak Caused by the Delta SARS-CoV-2 Variant. *medRxiv* [Preprint]. doi:10.1101/2021.07.07.21260122
- Long, Q. X., Liu, B. Z., Deng, H. J., Wu, G. C., Deng, K., Chen, Y. K., et al. (2020). Antibody Responses to SARS-CoV-2 in Patients with COVID-19. *Nat. Med.* 26, 845–848. doi:10.1038/s41591-020-0897-1
- Mahase, E. (2021a). Covid-19: Molnupiravir Reduces Risk of Hospital Admission or Death by 50% in Patients at Risk, MSD Reports. *BMJ* 375, n2422. doi:10.1136/bmj.n2422
- Mahase, E. (2021b). Covid-19: Pfizer's Paxlovid Is 89% Effective in Patients at Risk of Serious Illness, Company Reports. *BMJ* 375, n2713. doi:10.1136/bmj.n2713
- Malone, B., and Campbell, E. A. (2021). Molnupiravir: Coding for Catastrophe. *Nat. Struct. Mol. Biol.* 28, 706–708. doi:10.1038/s41594-021-00657-8
- Merck Sharp & Dohme Corp (2020). Efficacy and Safety of Molnupiravir (MK-4482) in Hospitalized Adult Participants with COVID-19 (MK-4482-001). [Online]. Available: <https://clinicaltrials.gov/ct2/show/NCT04575584> (Accessed 11 10, 2021).
- Merck (2021a). *Merck and Ridgeback Biotherapeutics Provide Update on Progress of Clinical Development Program for Molnupiravir, an Investigational Oral Therapeutic for the Treatment of Mild-To-Moderate COVID-19*. Available at: <https://www.merck.com/news/merck-and-ridgeback-biotherapeutics-provide-update-on-progress-of-clinical-development-program-for-molnupiravir-an-investigational-oral-therapeutic-for-the-treatment-of-mild-to-moderate-covid-19/> (Accessed November 10, 2021)
- Merck (2021b). *Merck and Ridgeback's Investigational Oral Antiviral Molnupiravir Reduced the Risk of Hospitalization or Death by Approximately 50 Percent Compared to Placebo for Patients with Mild or Moderate COVID-19 in Positive Interim Analysis of Phase 3 Study*. Available at: <https://www.merck.com/news/merck-and-ridgebacks-investigational-oral-antiviral-molnupiravir-reduced-the-risk-of-hospitalization-or-death-by-approximately-50-percent-compared-to-placebo-for-patients-with-mild-or-moderate/> (Accessed November 10, 2021)
- Painter, G. R., Bowen, R. A., Bluemling, G. R., Debergh, J., Edpuganti, V., Gruddanti, P. R., et al. (2019). The Prophylactic and Therapeutic Activity of a Broadly Active Ribonucleoside Analog in a Murine Model of Intranasal Venezuelan Equine Encephalitis Virus Infection. *Antivir. Res* 171, 104597. doi:10.1016/j.antiviral.2019.104597
- Painter, W. P., Holman, W., Bush Jim, A., Almazedi, F., Malik, H., Eraut Nicola, C. J. E., et al. (2021). Human Safety, Tolerability, and Pharmacokinetics of Molnupiravir, a Novel Broad-Spectrum Oral Antiviral Agent with Activity against SARS-CoV-2. *Antimicrob. Agents Chemother.* 65, e02428–02420. doi:10.1128/aac.02428-20

- Pastor-Anglada, M., and Pérez-Torras, S. (2018). Emerging Roles of Nucleoside Transporters. *Front. Pharmacol.* 9, 606. doi:10.3389/fphar.2018.00606
- Perez, M., Abuin, P., Actis, M., Ferramosca, A., Hernandez-Vargas, E. A., and Gonzalez, A. H. (2021). Optimal Control Strategies to Tailor Antivirals for Acute Infectious Diseases in the Host. *arXiv* [Preprint]. Available at: <https://arxiv.org/abs/2106.09528>.
- Planas, D., Veyer, D., Baidaliuk, A., Staropoli, I., Guivel-Benhassine, F., Rajah, M. M., et al. (2021). Reduced Sensitivity of SARS-CoV-2 Variant Delta to Antibody Neutralization. *Nature* 596, 276–286. doi:10.1038/s41586-021-03777-9
- Rambaut, A., Loman, N., Pybus, O., Barclay, W., Barrett, J., Carabelli, A., et al. (2020). *Preliminary Genomic Characterisation of an Emergent SARS-CoV-2 Lineage in the UK Defined by a Novel Set of Spike Mutations*. COVID-19 Genomics Consortium UK CoG-UK. Available at: <https://virological.org/t/preliminary-genomic-characterisation-of-an-emergent-sars-cov-2-lineage-in-the-uk-defined-by-a-novel-set-of-spike-mutations/563> (Accessed October 2021).
- Ridgeback Biotherapeutics (2020). Clinical Study Protocol: A Randomized, Double-Blind, Placebo-Controlled, First-In-Human Study Designed to Evaluate the Safety, Tolerability, and Pharmacokinetics of EIDD-2801 Following Oral Administration to Healthy Volunteers. [Online]. Available: [https://clinicaltrials.gov/ProvidedDocs/19/NCT04392219/Prot\\_000.pdf](https://clinicaltrials.gov/ProvidedDocs/19/NCT04392219/Prot_000.pdf) (Accessed 11 12, 2021 2021).
- Rosenke, K., Hansen, F., Schwarz, B., Feldmann, F., Haddock, E., Rosenke, R., et al. (2021). Orally Delivered MK-4482 Inhibits SARS-CoV-2 Replication in the Syrian Hamster Model. *Nat. Commun.* 12, 2295. doi:10.1038/s41467-021-22580-8
- Siemieniuk, R. A., Bartszko, J. J., Ge, L., Zeraatkar, D., Izcovich, A., Kum, E., et al. (2020). Drug Treatments for Covid-19: Living Systematic Review and Network Meta-Analysis. *BMJ* 370, m2980. doi:10.1136/bmj.m2980
- Tegally, H., Wilkinson, E., Giovanetti, M., Iranzadeh, A., Fonseca, V., Giandhari, J., et al. (2020). Emergence and Rapid Spread of a New Severe Acute Respiratory Syndrome-Related Coronavirus 2 (SARS-CoV-2) Lineage with Multiple Spike Mutations in South Africa. *medRxiv* [Preprint]. doi:10.1101/2020.12.21.20248640
- van Pruijzen, H. C., Vierwinden, G., Wessels, J., and Haanen, C. (1977). Cytosine Arabinoside Binding to Human Plasma Proteins. *Arch. Int. Pharmacodyn Ther.* 229, 199–205.
- Wahl, A., Gralinski, L. E., Johnson, C. E., Yao, W., Kovarova, M., Dinnon, K. H., et al. (2021). SARS-CoV-2 Infection Is Effectively Treated and Prevented by EIDD-2801. *Nature* 591, 451–457. doi:10.1038/s41586-021-03312-w
- Wang, W., Xu, Y., Gao, R., Lu, R., Han, K., Wu, G., et al. (2020). Detection of SARS-CoV-2 in Different Types of Clinical Specimens. *JAMA* 323, 1843–1844. doi:10.1001/jama.2020.3786
- Wang, R., Chen, J., Gao, K., and Wei, G. W. (2021). Vaccine-escape and Fast-Growing Mutations in the United Kingdom, the United States, Singapore, Spain, India, and Other COVID-19-Devastated Countries. *Genomics* 113, 2158–2170. doi:10.1016/j.ygeno.2021.05.006
- Yoon, J. J., Toots, M., Lee, S., Lee, M. E., Ludeke, B., Luczo, J. M., et al. (2018). Orally Efficacious Broad-Spectrum Ribonucleoside Analog Inhibitor of Influenza and Respiratory Syncytial Viruses. *Antimicrob. Agents Chemother.* 62, e00766–00718. doi:10.1128/AAC.00766-18
- Young, B. E., Ong, S. W. X., Kalimuddin, S., Low, J. G., Tan, S. Y., Loh, J., et al. (2020). Epidemiologic Features and Clinical Course of Patients Infected with SARS-CoV-2 in Singapore. *JAMA* 323, 1488–1494. doi:10.1001/jama.2020.3204

**Conflict of Interest:** The authors declare that the research was conducted in the absence of any commercial or financial relationships that could be construed as a potential conflict of interest.

**Publisher's Note:** All claims expressed in this article are solely those of the authors and do not necessarily represent those of their affiliated organizations, or those of the publisher, the editors and the reviewers. Any product that may be evaluated in this article, or claim that may be made by its manufacturer, is not guaranteed or endorsed by the publisher.

Copyright © 2022 Schöning, Kern, Chaccour and Hammann. This is an open-access article distributed under the terms of the Creative Commons Attribution License (CC BY). The use, distribution or reproduction in other forums is permitted, provided the original author(s) and the copyright owner(s) are credited and that the original publication in this journal is cited, in accordance with accepted academic practice. No use, distribution or reproduction is permitted which does not comply with these terms.